15th Triennial World Congress, Barcelona, Spain

AN OBSERVER FOR RUNOUT OBSERVATION DURING TRACK SEEKING FOR THE TWO-ACTUATOR OPTICAL DISK DRIVE

Jia-Yush Yen[1]
Professor

Gwo-Huei Wu[2]
Engineer

[1]Department of Mechanical Engineering,
National Taiwan University,
Taipei, Taiwan 10617, R.O.C.,
Tel: +886-2-2366-0734, Fax: +886-2-2366-0734
e-mail: jyen@ccms.ntu.edu.tw,
[2]Optical Research Laboratory
Industrial Technology Research Institute
Shinchu, Taiwan R.O.C.

Abstract: Runout observation in optical disk drive is a common research interest, but very few researches were able to address the runout problem during the track seeking process. This study investigated the possibility of using an on-line observer to estimate the disk runout during track accessing. A model based feedback algorithm for the track-accessing servo is used as the base for the design. The observer in the controller not only helps to provide the necessary feedback information during accessing, but also made it possible to measure the disk runout in the removable media. The experimental results showed that proper tuning of the controller clearly provide the track wobbling information that will make possible further investigation on how to eliminate the runout effect in the accessing process. *Copyright © 2002 IFAC*

Keywords: Observer, Optical Data Storage, Disk Oscillation, Disturbance Signals, Optimal Filtering.

1. INTRODUCTION

This paper studies the effect of disk runout on the optical disk drive track accessing. An on-line observer is designed that is able to perform on-line disk runout observation during track accessing. This observer will enable the controller to take into consideration the runout effect during accessing.

Track accessing is an important process in the disk drive operation. Most random access disk drives spent almost half of its operation time moving the data head across different tracks. The disk runout effect in a Winchester type hard disk drive is not obvious because the servo-write process will usually counter the runout action and creates concentric data tracks on the disks. The optical disk dive, on the other hand, has removable media, and the amount of runout is subject to each time the disk is inserted into the cartridge. The runout in these systems can thus be very severe. In addition, the data head in the optical drive contains the necessary optics (Imaino and Bhushan, 1991, Hitani and Tsunoda, 1984). It is heavier than the head in the other types of storage devices; the access time is also longer and is one of the major obstacles in its progress. Shortening the time can thus results in significant improvement in the drive performance.

The optical disk drive uses two-actuator solution: a fine actuator for the high resolution and a sled actuator to cover the large seek distance. For economic reason, the sled actuator is usually made of very crude plastic gearing driven by low cost DC motors, and the fine actuator is usually made of voice coil and leaf spring suspensions. This configuration allows for very fine track resolution, but it also introduces all kinds of undesirable nonlinear factors into its mathematical model (Kaneko, 1987). There are many results in the literature on the track-following control algorithms (Yen, et. Al., 1990, Soner, 1986a, Soner, 1986b, McCormick and Horowitz, 1991,Yang and Pei, 1996), but because of the double actuator nature of the optical head, very few has addressed the track accessing problem. McCormick and Horowitz (1991) adopted a

simplified model with two independent double integer plants to obtain an approximated analytical solution. Yang and Pei (1996) further discussed the detailed behaviour of the fine actuator for long track jump. Their main claim is that the control effort in the zero input periods should actually be a linear proportional effort. Basically, there is no result available on dealing with the track runout.

In this paper, the authors studied the effect of the disk runout. The result shows that a properly designed filter for the dual actuator system is able to distinguish between the fine actuator vibration and the disk runout. Thus, the filter is able to provide the runout information during the accessing process. It is than necessary to modify the track-accessing strategy. Experimental results show that if the velocity of the target track can be predicted, it is possible to modify the track accessing strategy to improve the settling characteristics.

The reset of this paper is divided as followings: The next section constructs the plant mathematical model that will be used throughout the paper. The model includes the coupling force between the sled and the fine actuator. Section 3 describes the track accessing servo and some of the problems encountered. Section 4 proposes an online observer for the disk runout during track accessing. Section 5 presents the experimental results and some discussions. Finally, section 6 presents the conclusions.

2. SYSTEM MODELING

Two stage actuators are adopted by almost all the commercial optical disk drives like CD players and DVD players to accomplish both high precision track following and long track seeking requirement.

Figure 1 shows the experimental TAODD actuator assembly. The actuator consists of a sled made of ball screw and DC motor with long stroke capability and a fine actuator with precise motion capability. Such dual actuator structure in the CD-ROM drive can accomplish as many as 45,000 tracks jumping and as precise as 0.16 mm positioning.

Figure 2 depicts the simplified mathematical model. The system shows a coupling effect from the acceleration of sled to fine actuator input. Generally the mass, M_s, of the sled is larger than that of the fine actuator. It should be noted that the equilibrium point for the fine actuator is defined at the central point of its travel. M_s in figure 1 is the mass of the sled, and x_s, the position of the sled, is measured absolutely to the global coordinate system and x_f, the position of the fine actuator, is measured relatively with respect to the equilibrium point.

Several assumptions have been made before the derivation of this model: (1) The sled consists of a dc motor in nature and is assumed to have a second order dynamic relation between the input voltage to output velocity, (2) The reaction force from sled to fine actuator is considered while the reaction force from fine actuator to sled is ignored since sled has larger mass than fine actuator.

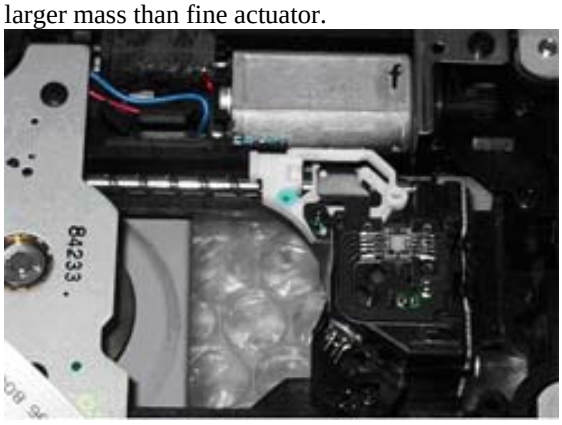

Figure 1. The two-actuator optical disk drive

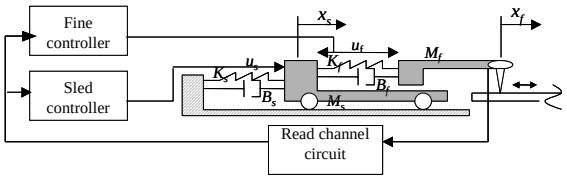

Figure 2. The basic structure of a two-actuator optical disk drive

The mathematical model can be further written in the state space form as:

$$\begin{bmatrix} x_1 \\ x_2 \\ x_3 \\ x_4 \\ x_5 \end{bmatrix} = \begin{bmatrix} 0 & 1 & 0 & 0 & 0 \\ 0 & 0 & 1 & 0 & 0 \\ 0 & -c_s & -b_s & 0 & 0 \\ 0 & 0 & 0 & 0 & 1 \\ 0 & 0 & -1 & -c_f & -b_f \end{bmatrix} \begin{bmatrix} x_1 \\ x_2 \\ x_3 \\ x_4 \\ x_5 \end{bmatrix} + \begin{bmatrix} 0 & 0 \\ 0 & 0 \\ g_s & 0 \\ 0 & 0 \\ 0 & g_f \end{bmatrix} \begin{bmatrix} u_1 \\ u_2 \end{bmatrix} \quad (1)$$

where x_1 is defined as the absolute position of sled (i.e. p_s in figure 2) , x_2 is defined as the absolute velocity of the sled, x_3 is defined as the absolute acceleration of sled, x_4 is the relative position of fine actuator with respect to the equilibrium point, and x_5 is the relative velocity of fine actuator. In this paper we adopt a test CD-ROM drive manufactured by Hitachi [10] and use laser interferometer for the identification measurement. And values of the coefficients for that drive are b_s is -621, c_s is -34268, b_f is -62, c_f is -22435, g_s is $2.71\text{x}10^6$ and g_f is $3.88\text{x}10^4$. The units of the variables are: x1 is in mm, x_2 is in mm/s, x_3 is in mm/s^2, x_4 is in mm, x_5 is in mm/s, u_1 and u_2 are in volts.

Figures 3 and 4 are the frequency response for the sled and the fine actuators, respectively. In figure 3, the input is the control, u1, with unit of volts and output is the position, x1, of sled with unit of mm. In figure 4, the input is the control, u2, in volts and output is the relative position, x4, in mm. Figure 4 also shows that the fine actuator has a resonance peak at a frequency about 30Hz. Figure 5 is the frequency response for the coupling effect worked on the fine actuator from sled, which shows from gain plot that the gain is less than 1 and can be easily eliminated by fine actuator itself.

3. THE TRACK ACCESSING SERVO

The optical disk drive servo system takes charge of several necessary functions to enable data accessing from the optical disk. First of all, a focusing servo focuses the laser beam on the disk surface to bounce off the correct optical signal back to the light processing circuit. Secondly, a track-following servo will read the servo-tracking signal to keep the data head on track. Thirdly, the spindle motor will keep the disk spinning at designated rate to allow correct interpretation of the read back data. Finally, the track-accessing servo kicks in when there is need to access a different track.

The track-accessing strategy is usually based on the classical time-optimal control strategy. As mentioned before, the two-actuator MIMO time-optimal control solution is difficult to obtain. Therefore it is custom instead to use single actuator solution for the sled and try to lock the fine actuator in a neutral position to accommodate for the target track movement. That is to use a maximum acceleration profile for the acceleration phase until the velocity reaches the velocity limit, and then to curse at constant velocity until a maximum deceleration curve will lead the system to the target. As the head moves close to the target track, the servo system switches to the track-following servo and lock on to the target track. The final phase of this accessing process is difficult because the transition between the two servo strategies induces mismatches in the initial conditions. The target track movement results in a change in the predicted travelling distance and final state conditions. Excessive overshoot may occur and lead to very long settling or track skip. In addition, the fine actuator oscillation from the sled motion can make it even harder for the head to lock on the moving target track.

To deal with this problem, Yen (1999) has suggested that the fine actuator should maintain high damping characteristic during accessing to suppress the oscillation induced by the sled movement. The target track movement is seldom addressed because it is necessary to be able to tell what the target is doing before one can actually do anything with it. In the next section, we will propose an on-line observer that is aimed at observing the disk wobble as a way to provide access the target track behaviour

.

4. ON-LINE OBSERVER FOR DISK WOBBLE

Neglecting the coupling effect between the sled and the fine actuator, the sled and fine accessing control loops become:

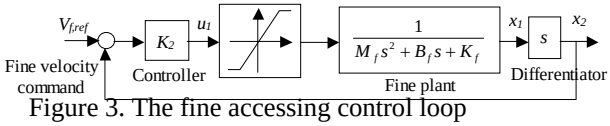

Figure 3. The fine accessing control loop

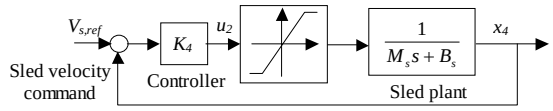

Figure 4. The sled accessing control loop

The closed-loop transfer function for the fine and sled control loops becomes:

$$\frac{x_2}{v_{f,ref}} = \frac{k_2 s}{M_f s^2 + (B_f + k_2)s + K_f}$$

$$\frac{x_4}{v_{s,ref}} = \frac{k_4}{M_s s + (B_s + k_4)}.$$

The state space representation of the discrete system then can be expressed as:

$$\mathbf{x}_{k+1} = \Phi_k \mathbf{x}_k + \Gamma_k \mathbf{u}_k + \mathbf{G}_k w_k$$

$$y_k = \mathbf{H}_k \mathbf{x}_k + v_k .$$

The observer is defined as

$$\hat{\mathbf{x}}_{k+1} = \Phi_k \hat{\mathbf{x}}_k + \Gamma_k \mathbf{u}_k + \mathbf{L}_k (y_k - \hat{y}_k)$$

where $\hat{y}(k) = \mathbf{C}\hat{\mathbf{x}}(k)$. From classical control theory, it is possible to place the observer poles to modify the observation characteristics.

In the TAODD, the fine actuator has a high bandwidth response while the sled is intrinsically low bandwidth. Thus, the state observer for the fine actuator should have a fast response to capture the high frequency tracking error. The sled observer, on the other hand, probably should not have very fast frequency response. In the experiment, a Kalman filter with artificial noise covariance is designed to achieve this goal.

Assuming that the noises are zero mean and uncorrelated, and assume the initial conditions: $\mathbf{P}_0 = \mathbf{P}_{x_0}$, $\hat{\mathbf{x}}_0 = \bar{\mathbf{x}}_0$. It is possible to calculate the Kalman filter gains through a coupled procedures []:

Sequence update:

The error covariance: $\mathbf{P}_{k+1}^- = \Phi_k \mathbf{P}_k \Phi_k^T + \mathbf{G}_k \mathbf{Q}_k \mathbf{G}_k^T$,

State estimation: $\hat{\mathbf{x}}_k^- = \Phi_k \hat{\mathbf{x}}_k + \Gamma_k \mathbf{u}_k$

Measurement update:

Error covariance: $\mathbf{P}_{k+1} = \left[\left(\mathbf{P}_{k+1}^- \right)^{-1} + \mathbf{H}_{k+1}^T \mathbf{R}_{k+1}^- \mathbf{H}_{k+1} \right]^{-1}$

State estimation:

$\hat{\mathbf{x}}_{k+1} = \hat{\mathbf{x}}_{k+1}^- + \mathbf{P}_{k+1} \mathbf{H}_{k+1}^- \mathbf{R}_{k+1}^- \left(y_{k+1} - \mathbf{H}_{k+1} \hat{\mathbf{x}}_{k+1}^- \right)$

Compare with the Kalman filter, the filter gain is defined by $\mathbf{L}_k = \mathbf{P}_k \mathbf{H}_k^T \mathbf{R}_k^-$.

The disturbance of the system mainly arises from the track runout, which is typically 87 tracks from the optical head datasheet. Thus the value of **R** is set to $87^2 = 7569$. The value of the matrix **Q** determines the observer bandwidth. A very small **Q** results in small observer bandwidth and should better reflect the true system behaviour; however, the low bandwidth loop usually results in sloppy performance and can lead to difficulties in track locking. A large **Q** may lead to inaccurate state estimation, but it may also provide better noise suppression. The experiment finally reached the following values of **Q** = $\begin{bmatrix} 7\times10^6 & 0 \\ 0 & 7\times10^7 \end{bmatrix}$ to be a good choice. Figure 5 is a frequency of the resulted close-loop frequency response for the fine actuator. Figure 6 is the close-loop frequency response for the sled. One easily sees that the fine actuator can track error up to very high frequency. On the other hand, the sled control loop only has very low bandwidth capability.

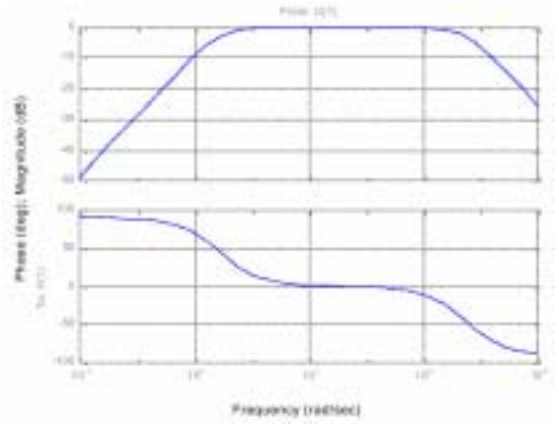

Figure 5. Fine observer frequency response.

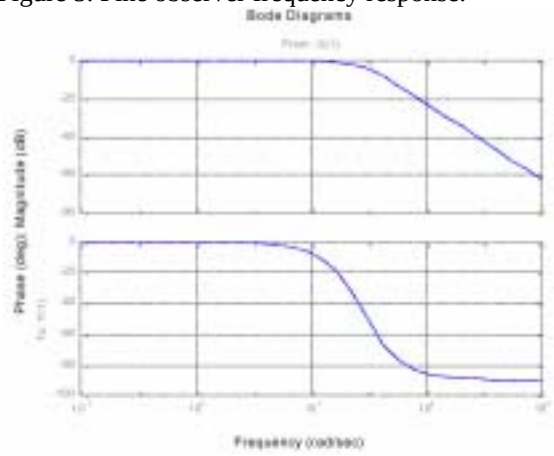

Figure 6. Sled actuator closed-loop frequency response

5. EXPERIMENTAL RESULTS AND DISCUSSIONS

5.1Parameter Settings

The experimental settings are:

Maximum speed v_{max}	200,000 tracks/s	
Maximum acceleration a_{max}	1.115398x10^7 tracks/s^2	
Fine gain K_2	Constant velocity region	0.000005
	Deceleration region	0.000035
Sled gain K_4	0.0003	
Spindle speed	18X	
Fine saturation voltage	1.8V	
Sled saturation voltage	1.8V	

Table 1 Parameter Setting

The numbers are experimentally determined for suitable performance.

5.2 Runout Observation

The following experiments use the observer designed in the last session to study the runout on the optical. First the system is tested for 18 times drive speed. The signals in figures 7-1 and 7-2 are:
Channel 4: TE (the tracking error signal),
Channel 3: Seek interval,
Channel B: Track settling process (Track-following starts when the signal turns low. Locking completes when the signal turns back high again.)
Channel D: Closer look at the TE signal.

Figures 7-3 shows the velocity portrait of the sled and fine actuators. Comparing figures 7-2 and 7-3, the observed find runout velocity is a little bit higher than the actual measured value, while the sled obviously does not follow the runout motion. The result matches the original design goal to using the fine actuator for the runout and leave the sled unaffected. Figure 7-4 shows the estimated and actual optical head position. It shows not only a periodical runout signal as expected, it is also an indication that the observer is capable of reflecting the needed runout signal.
Figures 8-1, 8-2, 9-1, 9-2, 10-1 and 10-2 shows the runout observation of disk drive running at 4, 8 and 24 times drive speed. Some of the observations are made:
1. First of all, runout can be characterized as a periodic oscillation whose frequency is proportional to the spindle speed but whose amplitude remains relatively unchanged.
2. The fine actuator literal velocity is around ± 2×104 (tracks/sec) at 4 times drive speed, while the sled moves at ± 2000 (tracks/sec). When the drive reaches 24 times drive speed, the fine can get ± 7×104 (tracks/s), and the sled becomes ± 5000 (tracks/s). That is the wobble velocity of the actuators also increases with increasing spindle speed.
3. The estimated speed is a little bit larger than the actual speed. This can be fixed by lowering the Kalman filter gain; however, this can also cause the position estimation to increase.
4. The position estimation seems to drift with time. This can arise from a bias voltage that has to be applied to the fine actuator.

6. CONCLUSIONS

This paper designed an on-line observer to estimate the disk runout during track accessing. The observer is base on the Kalman filtering technology and is basically easily implemented. Experimental results show that the observer is able to identify the track runout from the random tracking error signal and provide the servo system with an access to the track runout for future runout suppression controller design.

7. ACKNOWLEDGEMENTS

This work is a cooperative effort between the Opto-Electronics & Systems laboratories of the Industrial Technology Research Institute, Taiwan Hsinchu and the National Taiwan University under contract No. 89S17-J4, and is supported in part by National Science Council, ROC under project no. NSC89-2213-E-002-144.

8. REFERENCES

Imaino,W., and Bhushan,B., 1991, “Actuation Mechanisms in optical storage”, Advances in information storage systems, vol.1, pp.375-404.

Jennings, L.S., Fisher, M.E., Teo, K.L., and Goh, C.J., 1995, "MISER3 Optimal control software," Theory and User Manual, Ver. 2.0.

Kaneko,R., 1987, "Magnetic and optical disk storage technology", JSME International Journal, Vol.30, No.260, Feb., pp.215-220.

Kaya, C.Y. and Noakes, J.L., 1996, Computations and time-optimal controls, Chichester, Engl John Wiuley & Sons Ltd.

Kitani,H., and Tsunoda,Y., 1984, "Large-capacity optical disk files", Hitachi review, Vol.33, No.3, pp.109-114.

McCormick,J. and Horowitz,R., 1991, "Time Optical Seek Trajectories for a Dual Stage Optical Disk Drive Actuator," ASME J. of Dynamic Systems, Measurement, and Control, Vol.113, Sep., pp.534-536.

Meszaros, C., 1996, "The efficient implementation of interior point methods for linear programming and their applications," Ph.D. Thesis, Eotvos Lorand University of Sciences, Ph.D. School of Operations Research, Applied Mathematics and Statistics, Budapest.

Mitsuya,Y. and Takanami,S., 1987, "Technologies for high recording density in large-capacity fast-access magnetic disk stroage," IEEE Trans. on Magnetics, Vol.MAG-23, No.5, Sep.

Rao, S.S., 1996, Engineering optimization: theory and practice, 3rd edition, John Wiley & Sons, Inc.

Soner,H.M., 1986, "Optimal control with state- space constraint I", SIAM J. control and optimization, Vol.24, No.3, May, pp.552-561.

Soner,H.M., 1986, "Optimal control with state- space constraint II", SIAM J. control and optimization, Vol.24, No.6, Nov., pp.1110-1122.

Tohei Co., 1996, Specifications of TCR-M12, Tohei Industrial Co., Ltd.

Yang, J.-D. and Pei, X.-D., 1996, "Seek time and trajectories of time optimal control for a dual stage optical disk drive actuator," IEEE Transactions on Magnetics, Vol.32, No.5, Sep., pp.3857-3859.

Yen.J.Y., Hallamasek,K., and Horowitz,R., 1990, "Track-following controller design for a compound disk drive actuator", ASME Trans. J. of Dynamic Systems, Measurement, and Control, Vol.112, Sep., pp.391-402.

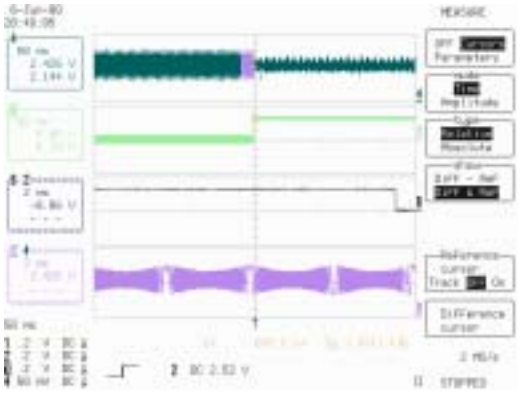

Figure 7-1. Track accessing signals under 18 times speed

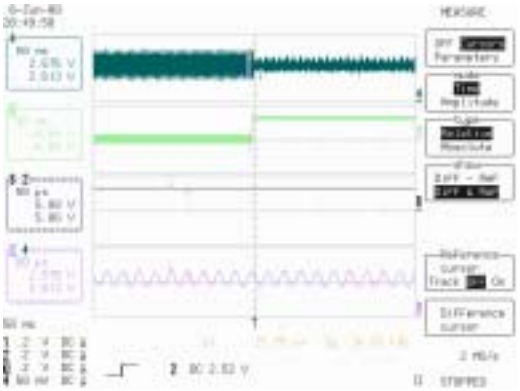

Figure 7-2. Amplified signals to observe the runout signal under 18 times speed

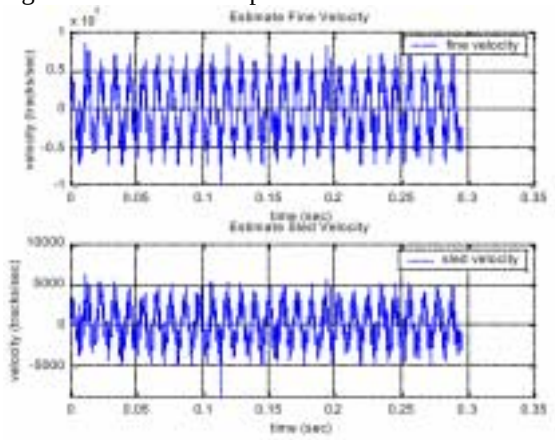

Figure 7-3 Runout velocity estimation for disk drive under 18 times speed

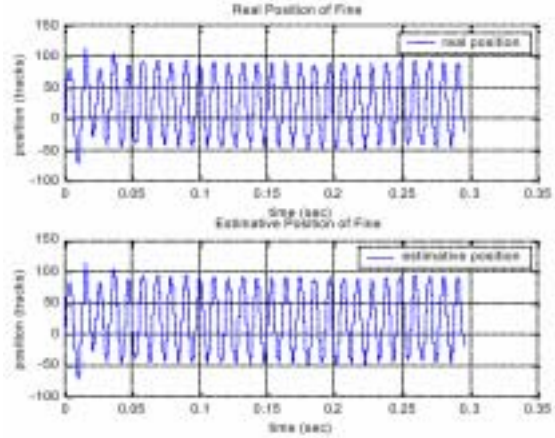

Figure 7-4. The actual and estimated head position under 4 times speed

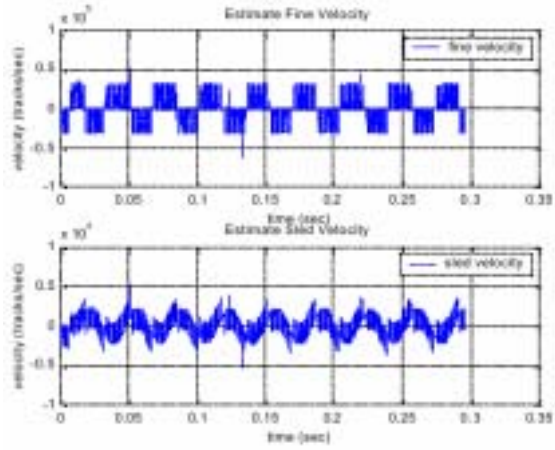

Figure 8-1 Runout velocity estimation for disk drive under 4 times speed

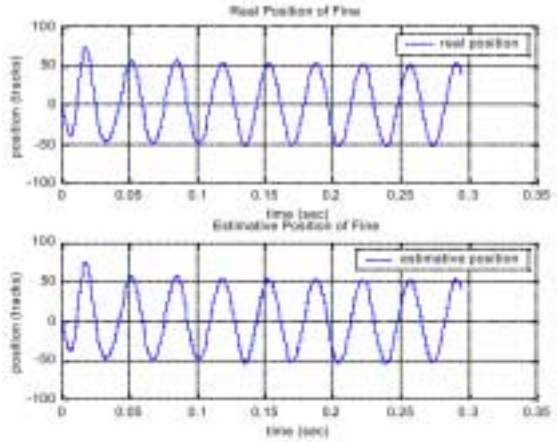

Figure 8-2. The actual and estimated head position under 4 times speed

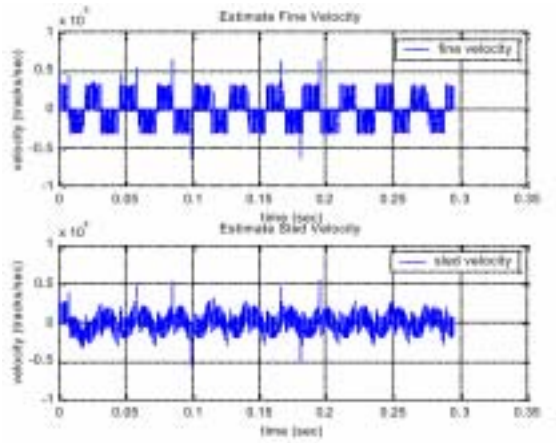

Figure 9-1 Runout velocity estimation for disk drive under 8 times speed

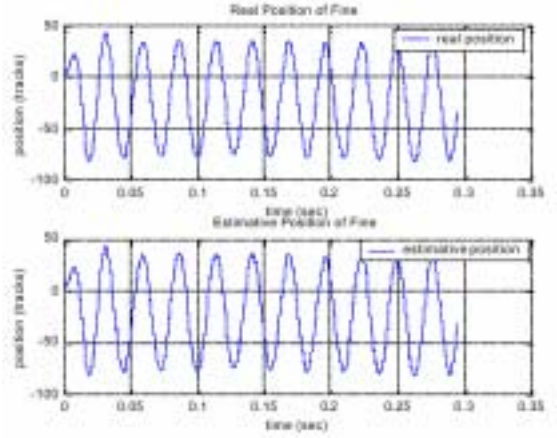

Figure 9-2. The actual and estimated head position under 8 times speed

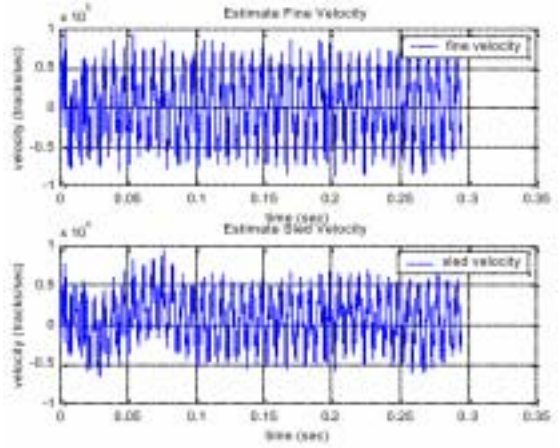

Figure 10-1 Runout velocity estimation for disk drive under 24 times speed

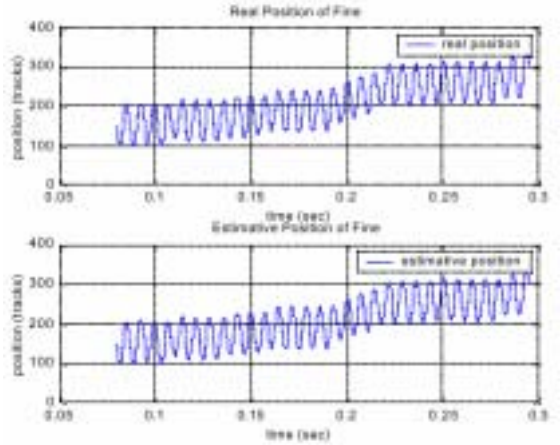

Figure 10-2. The actual and estimated head position under 24 times speed